Carbohydrate Polymers 96 (2013) 466–473

Contents lists available at SciVerse ScienceDirect

Carbohydrate Polymers

journal homepage: www.elsevier.com/locate/carbpol

# Structure and anti-inflammatory capacity of peptidoglycan from *Lactobacillus acidophilus* in RAW-264.7 cells

Zhen Wu [a], Dao-dong Pan [a,b,*], Yuxing Guo [a], Xiaoqun Zeng [b]

[a] Food Science & Nutrition Department, Nanjing Normal University, Nanjing 210097, PR China
[b] Food Science and Technology Department of Marine Science School, Ningbo University, Ningbo 315211, PR China

ARTICLE INFO

*Article history:*
Received 9 February 2013
Received in revised form 25 March 2013
Accepted 10 April 2013
Available online 18 April 2013

*Keywords:*
PGN
*L. acidophilus*
HPLC
Structure analysis
Anti-inflammatory capacity

ABSTRACT

Probiotic bacteria, especially the *Lactobacillus* species, can potentially play a significant role in the antiviral and antimicrobial activity of a host's immune system. *Lactobacillus acidophilus*, an intestinal bacterium, is involved in the intestinal epithelial cell response when a pathogen adheres to a cell. In this study, the structure of peptidoglycan (PGN) isolated from *L. acidophilus* was determined with the help of HPLC, NMR, FT-IR and MALDI-TOF/TOF MS. The molecular mass of PGN is 875.260 Da. The anti-inflammatory capacity of PGN was evaluated in model RAW 264.7 cells. Epifluorescence microscopy images and western blot analysis provided compelling evidence of PGN's anti-inflammatory capacity on LPS-induced macrophages. A significant decrease in inducible NO synthase (iNOS) and cyclooxygenase-2 (COX-2) levels when PGN was added up to 200 μg/ml. These data provide new insight into the cellular and molecular mechanisms by which probiotic bacteria can contribute to maintaining good health.



## 1. Introduction

Intestinal bacteria, such as *Lactobacillus*, *Bifidobacterium, Lactococcus* and *Streptococcus* spp., have received considerable attention as examples of probiotic microorganisms (Florez et al., 2008). Lactic acid bacteria (LAB) are estimated to consist of at least 400 different species, of which many are associated with the human gastrointestinal tract. *Lactobacillus* species, such as *Lactobacillus acidophilus, Lactobacillus delbrueckii* subsp. *Bulgaricus*, *Lactobacillus casei* and *Lactobacillus rhamnosus* have long been used in the manufacture of yogurt and cheese (Ng, Yeung, & Tong, 2011). LAB also exhibited antiviral activity when cell line models of animal and human intestine, and macrophages were challenged with rotavirus and transmissible gastroenteritis virus (Maragkoudakis, Chingwaru, Gradisnik, Tsakalidou, & Cencic, 2010). Several studies have demonstrated that *L. acidophilus* is a potential probiotic based on their immunomodulating activity by which they upregulate anti-inflammatory factors and thereby enhance immunity (Aly, Abdel-Galil Ahmed, Abdel-Aziz Ghareeb, & Mohamed, 2008; O'Flaherty & Klaenhammer, 2010).

*L. acidophilus* is a Gram-positive, non-spore forming rod, obligately homofermentative LAB that grows in anaerobic conditions. Though the effect of *L. acidophilus* on the modulation of host immunity has been shown by clinical evidence, the molecular and cellular mechanisms of these effects are not completely clear (Weiss et al., 2010). Molecular structures, such as peptidoglycan (PGN) and lipotechoic acid (LTA) of *L. acidophilus*, may be involved in the responses of intestinal epithelial cells (Ebrahimi & Jafarei, 2011; Vissers et al., 2010).

PGN, an amazing giant macromolecule (long glycan strands cross-linked by peptide side bridges), is an essential and specific component surrounding bacterial cells with a single covalent molecular sacculus, which is responsible for shape determination and cellular viability (Zapun, Noirclerc-Savoye, Helassa, & Vernet, 2012). The basic structure of PGN is polymers of alternating N-acetylglucosamine (NAG) and N-acetylmuramic acid (NAM) in (β-1,4) linkage, cross-linked by short peptide stems composed of alternating L- and D-amino acids. The structure of the PGN segment is the basis for a proposal for the structure of the bacterial cell wall polymer (Meroueh et al., 2006; Shah, Laaberki, Popham, & Dworkin, 2008). A classic model of PGN architecture from *Bacillus subtilis* suggests that glycan strands run parallel to the plasma membrane (Fig. 1), while the stem peptide varies depending on the bacterial species (Chaput & Boneca, 2007).

In Gram-negative bacteria, PGN is in a pathogen-associated molecular pattern, which is a potent activator of an innate immune response in the host. Some studies have demonstrated that Gram-negative bacteria, such as *Escherichia coli* and *S. flexner*, can stimulate the Nod1 pathway, whereas two Gram-positive PGNs do not (Girardin et al., 2003). Such effects have been attributed to

* Corresponding author at: Food Science & Nutrition Department,Nanjing Normal University,Nanjing 210097, PR China. Tel.: +86 0258 3598286; fax: +86 0258 3598901.
*E-mail address:* daodongpan@163.com (D.-d. Pan).

0144-8617/$ – see front matter © 2013 Elsevier Ltd. All rights reserved.
http://dx.doi.org/10.1016/j.carbpol.2013.04.028

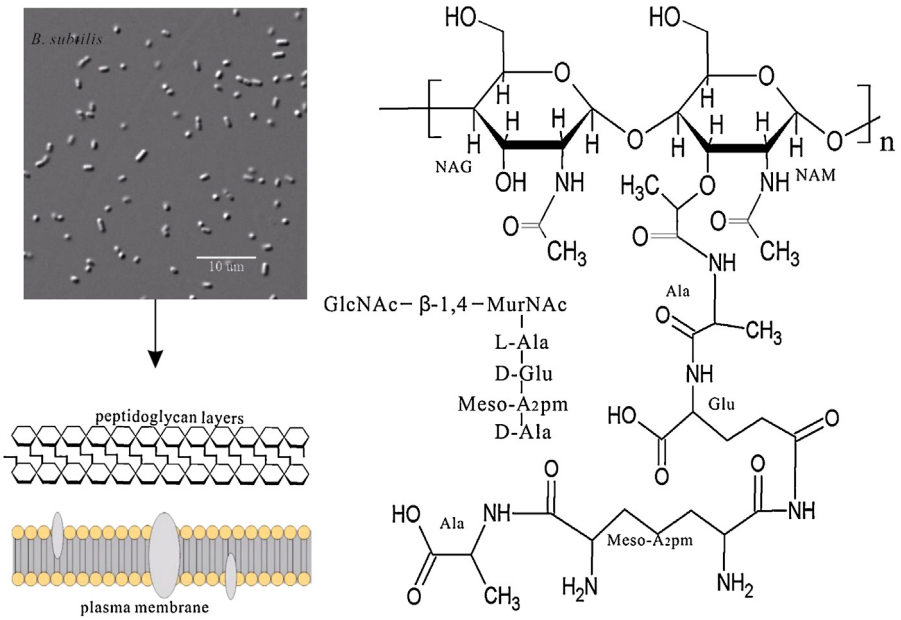


**Fig. 1.** Model peptidoglycan structure of *B. subtilis*.

the different PGN chemotypes at the third amino acid of the peptidic chain and to variations in the cross-bridge structure (Travassos et al., 2004).

Much attention has been focused on the Gram-negative bacteria PGN in relation to bacterial pathogens. Although PGNs are common to most biofilms, their matrix composition can vary greatly depending on the bacterial species (Hayhurst, Kailas, Hobbs, & Foster, 2008). Gram-positive bacteria contain a 20–80 nm thick cell wall with PGN accounting for 40–90% of its dry weight (Dworzanski, Tripathi, Snyder, Maswdeh, & Wick, 2005). Certain popular LAB strains are used in the food fermentation industry to improve safety, flavor, appearance, and texture, as well as to enhance food's physiologic and hygienic value (Semjonovs, Jasko, Auzina, & Zikmanis, 2008). It is important to determine whether PGNs isolated from LAB display a potent anti-inflammatory effect on pathogenic bacteria.

Among the strategies used to elucidate the structure of PGNs, chemical and biological approaches have led to their complete purification and structural characterization. Generally, biochemical analysis of PGN requires a hydrolysis process with a muramidase, resulting in release of muropeptide fragments. A dozen stem peptide structures have also been determined using an amidase (Atrih, Bacher, Allmaier, Williamson, & Foster, 1999). High-performance liquid chromatography (HPLC) and matrix-assisted laser desorption/ionization mass spectrometry techniques (MALDI-MS) have revealed a high level of PGN complexity in several species (Atrih, Zöllner, Allmaier, & Foster, 1996). Even with such knowledge, many issues remain unclear. Researchers have yet to determine how PGN is synthesized, modified and hydrolyzed, and how such changes relate to the stress-bearing capability of bacteria. The dynamic structure of PGN is also still largely obscure.

The present study sought to evaluate the structure of PGN isolated from *L. acidophilus*. We also explored the anti-inflammatory effects of PGN in a model macrophage cell line, RAW 264.7 to gain more details about probiotic bacteria and their effector molecules which contribute to their properties that promote good health.

## 2. Materials and methods

### 2.1. Reagents

DNase I, RNase A, trypsin, sodium dodecyl sulfate (SDS), calcofluor white (CFW, a compound that reacts with β-1,3 and β-1,4 carbohydrate linkages), and fluorescein isothiocyanate (FITC, an amine reactive derivative of fluorescein dye) were purchased from the Sigma–Aldrich Company (Shanghai, China). Antibody to iNOS, COX-2 and glyceraldehyde-3-phosphate dehydrogenase (GAPDH) were purchased from Cell Signaling Technology, and second antibodies were purchased from LI-COR Biosciences. Deionized water was purified in a Milli-Q plus system from Millipore prior to use. Other reagents were all of analytical reagent quality.

### 2.2. Strain and culture media

*L. acidophilus* was isolated from the gastrointestinal tract and identified by 16S rRNA analysis. The *L. acidophilus* strain was cultured in de Man–Rogosa–Sharpe (MRS) media, after which fresh media were inoculated with 1% (v/v). Cells were centrifuged at 5000 × *g* for 5 min at 4 °C. Pellets were harvested to isolate the PGN (McPherson & Popham, 2003).

### 2.3. Peptidoglycan isolation

Pellets (from 100 ml culture medium) isolated from exponential phase (16 h) cells were boiled for 30 min in 4% SDS. Suspensions were cooled at 4 °C, centrifuged at 6000 × *g* for 5 min at room temperature, and washed with distilled water until free of SDS. Pellets were processed using an ultrasonic processor (200 W, 3 × 99 times), and thrice washed with distilled water. The washed pellets were suspended in 10 ml of 100 mM Tris–HCl (pH 7.5) and incubated with DNase I (5 μl, 1 mg/ml), RNase A (5 μl, 5 mg/ml), and $MgSO_4$ (20 mM) at 37 °C for 2 h. Trypsin (10 μl, 10 mg/ml) and $CaCl_2$ (10 mM) were added and incubated at 37 °C for 12 h. Free of all the enzymes, the pellets were boiled in 1% SDS for 10 min SDS-insoluble cell wall material was washed until free of SDS and suspended in

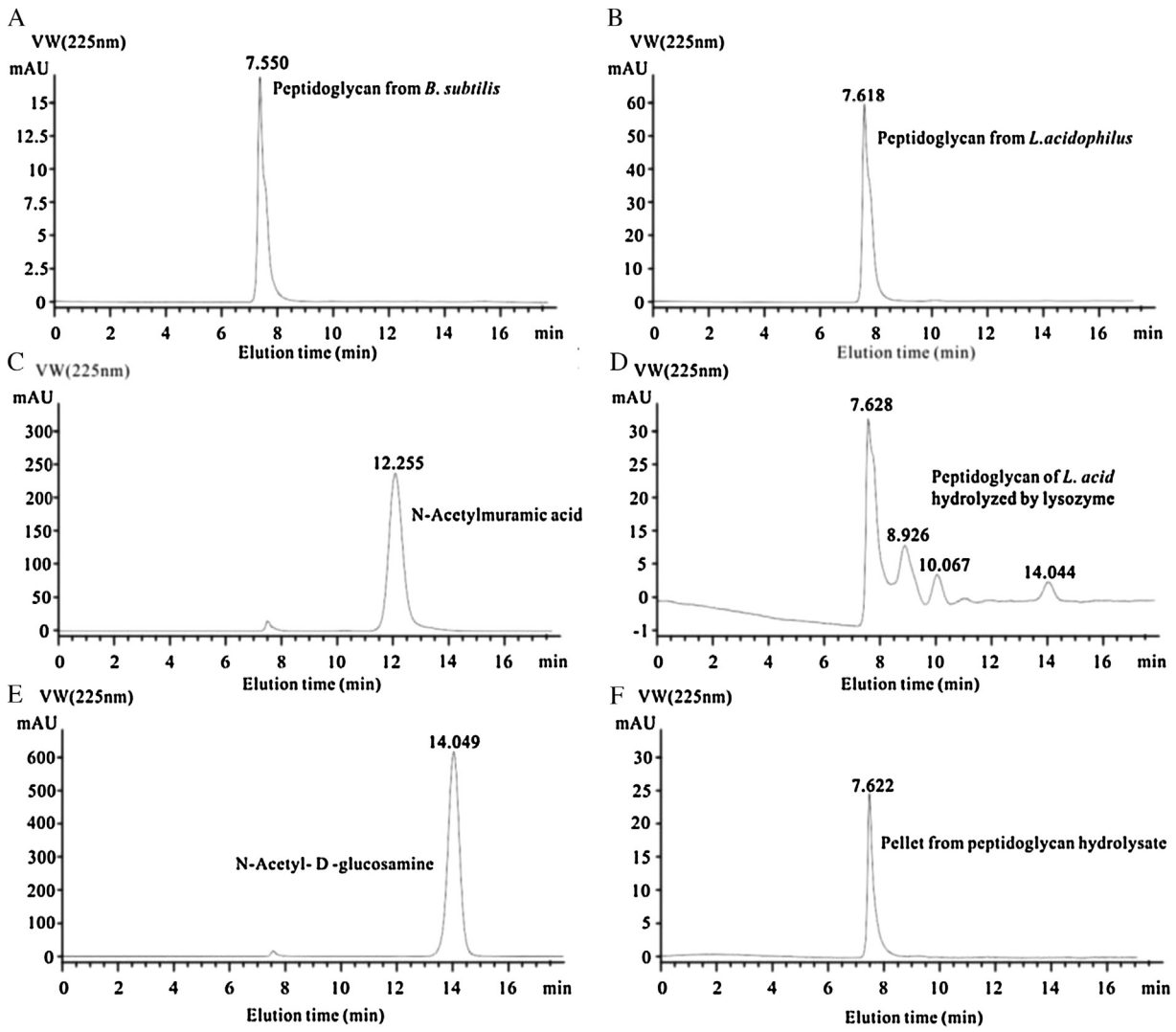


**Fig. 2.** HPLC profiles of PGN and PGN hydrolysates. (A) PGN of *B. subtilis*. (B) NAM on Aminex HPX-87H column. (C) NAG on Aminex HPX-87H column. (D) PGN of *L. acidophilus*. (E) Degradation supernatant products of PGN digested with muramidase. (F) Pellet products of PGN digested with muramidase.

trichloroacetic acid (10%) at 4 °C for 24 h to remove LTA. Water-insoluble material was then washed with cold distilled water until the pH was neutral. The PGN was collected and stored at −20 °C for further study (Atrih et al., 1999; Shah et al., 2008).

### 2.4. Soluble PGN analysis by HPLC and MS

Samples containing soluble PGN were separated with an Agilent HPLC system and an Aminex HPX-87H column from Bio-Rad (300 mm × 7.8 mm) and compared with retention times of known muropeptides from *B. subtilis*, a model organism for PGN study (McPherson & Popham, 2003). The column was equilibrated at 37 °C (throughout the experiment) at a flow rate of 0.5 ml/min with elution buffers ($H_2SO_4$, 5 mM) for 30 min. The flow rate was constant at 0.5 ml/min for 18 min after sample injection (20 μl). Soluble PGN was detected at 225 nm (Fig. 2). The eluted compounds were detected by monitoring $A_{225}$ (Meisen, Wingender, & Telgheder, 2008).

Soluble PGN was analyzed with MALDI-TOF/TOF MS (ultraflex TOF/TOF; Bruker Daltonics Inc., USA). One μl of each soluble PGN (filtered from 1 mg/ml PGN) was mixed with 1 μl of saturated 2,5-dihydroxybenzoic acid (DHB) matrix solution (50 mg/ml). A droplet of the resulting mixture (1 μl) was placed on the sample target and dried at room temperature. The sample was loaded into a mass spectrometer and analyzed (Chambery, del Monaco, Di Maro, & Parente, 2009).

The mid-infrared region (4000–400 $cm^{-1}$) Fourier Transform Infrared Spectroscopy (FT-IR) and nuclear magnetic resonance spectroscopy (NMR; this method was not as suitable for analysis of PGN's structure, given PGNs insolubility) were also used for the structural analysis of PGN.

### 2.5. Amino acid analysis of PGN

Different methods for analysis of amino acids have been developed and commercialized. PGN was hydrolyzed by 6 N HCl at 110 °C for 24 h. Analysis of PGN's amino acids was performed using an A200 Amino Nova amino acid analyzer (Physics and Chemistry Test Center, Jiangsu Province, China).

### 2.6. Microscopic observation of water-insoluble PGN

One of our goals was to verify the presence of NAG and NAM in PGN. Water-insoluble PGN was labeled with CFW and FITC (Calamita, Ehringer, Koch, & Doyle, 2001; Domenech, Garcia, Prieto,

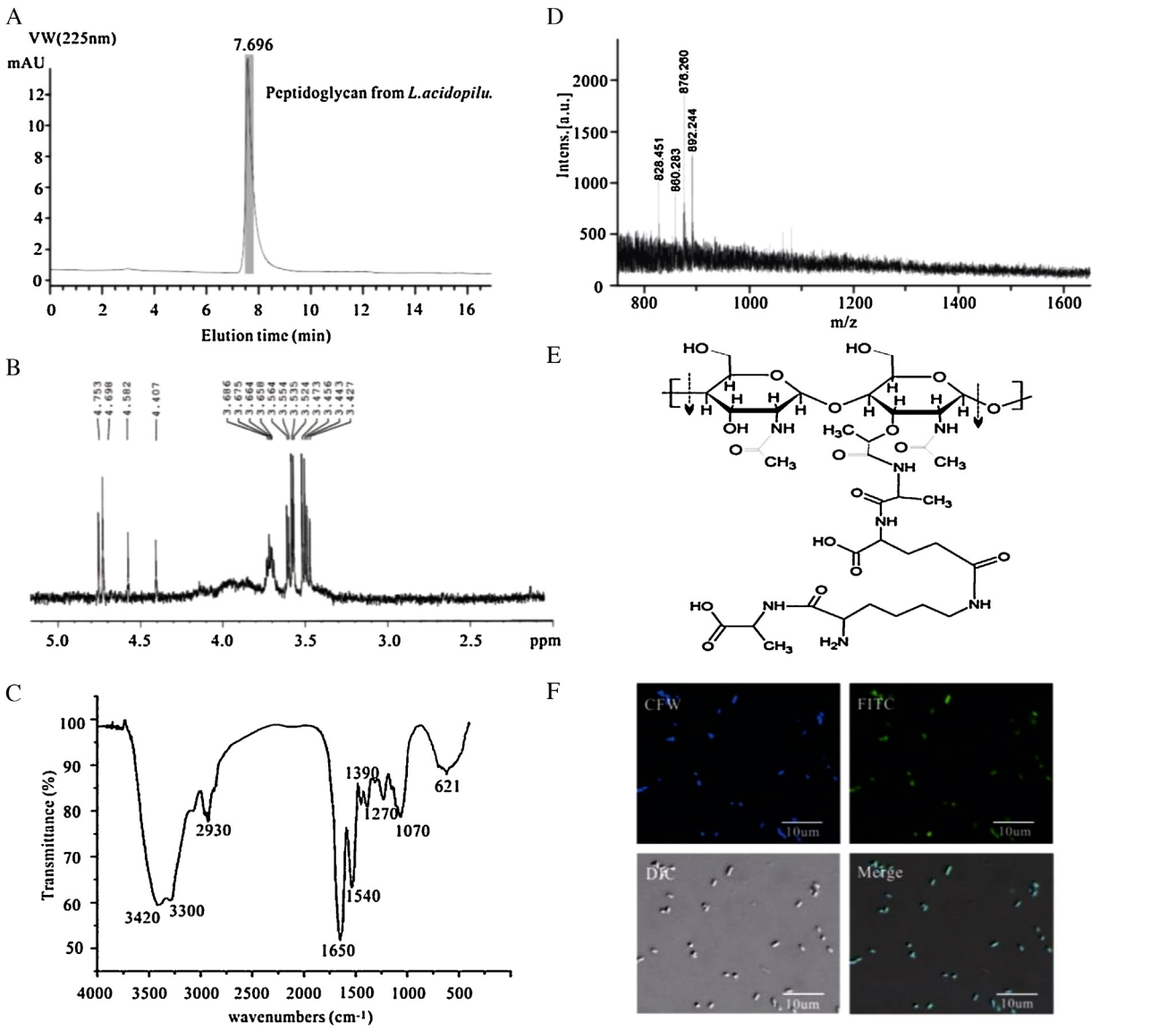


**Fig. 3.** Soluble PGN analyzed by different methods, and proposed PGN structures. (A) PGN of *L. acidophilus* identified on Aminex HPX-87H column. (B) $^{1}$H spectrum of PGN detected at 400 MHz on a Bruker Avance III NMR spectrometer. (C) Spectra of PGN in the mid-infrared region (4000–650 cm$^{-1}$). (D) Soluble PGN analyzed by MALDI-TOF/TOF MS. (E) Predicted structure of PGN from *L. acidophilus*. (F) Visualization of CFW- and FITC-labeled PGN sacculus images under 63× objective.

& Moscoso, 2012). Labeled PGN was then visualized using a Zeiss fluorescence microscope (Carl Zeiss, Inc., Jena, Germany).

### 2.7. Probiotic activity and dose dependency of PGN

The RAW 264.7 murine macrophage-like cell line model was used to investigate the probiotic activity of PGN. RAW 264.7 cells were seeded into 96-well plates ($2 \times 10^4$ cells/well). After 24 h, cells were treated with various concentrations of PGN sacculus (insoluble PGN). LPS (100 ng/ml) was added to stimulate cells 3 h later. Probiotic activity was determined by 3-(4,5-dimethylthiazol-2-yl)-2,5-diphenyltetrazolium bromide (MTT) assay and absorbance was detected at 570 nm to express the cells' viability (Kang et al., 2012).

The PGN-regulated, LPS-induced inducible NO synthase (iNOS) and cyclooxygenase-2 (COX-2) associated with inflammation were detected with western blot analysis (WB) (Shih, Cheng, Shen, & Cherng, 2010).

## 3. Results

### 3.1. PGN determined by HPLC on Aminex HPX-87H column

According to the method described previously, PGN of *L. acidophilus* was analyzed using HPLC on an Aminex HPX-87H column. Retention time (7.618 min) of natural PGN from *L. acidophilus* differed from the retention time (7.550 min) of known PGN from *B. subtilis* (Fig. 2A and D). Fig. 3E and F shows HPLC patterns of the degradation products of PGN digested with muramidase; NAG fragments (14.04 min) were observed in both figures. For NAM links to the peptide stem in PGN sacculus, NAM (12.255 min) did not appear in PGN hydrolysates, but did appear in two fractions at 8.926 min and 10.067 min.

### 3.2. PGN structure analysis

New methods and refinements of older approaches are leading to greater elucidation of the structure of PGN. Soluble PGN isolated

from *L. acidophilus* was analyzed by MALDI-TOF/TOF MS (Nanjing Normal University, China), FT-IR and NMR. Main *m*/*z* ratios of 828.451, 860.283 and 876.260 and 892.244 were obtained (Fig. 3D).

In amino acid analysis, 17 kinds of amino acid were detected using an A200 Amino Nova amino acid analyzer. Alanine (Ala), glutamic acid (Glu) and lysine (Lys) formed a significant part of the total amino acid component (data not shown).

### 3.3. Further characterization of PGN

The results for PGN sacculus isolated and purified from *L. acidophilus* and labeled with CFW and FITC are shown in Fig. 3F. The presence of β-1,4 carbohydrate linkages and Lys contributed significantly to the identification of the structure of PGN.

### 3.4. Dose-dependent manner of PGN acting on LPS-induced RAW 264.7 cell lines

For the insoluble character of PGN, a phagocytosis model was adopted on RAW 264.7 cells (Fig. 4). Phagocytosis of PGN sacculus by RAW 264.7 cells occurred when LPS was used to induce inflammation. The WB result also showed that iNOS and COX-2 changed in a dose-dependent manner related to PGN (Fig. 5). When the LPS-induced RAW 264.7 cells were compared, there was no significant difference between the PGN-treated and untreated RAW 264.7 cells (Fig. 6).

## 4. Discussion

The major structural polymer in the cell walls of most bacteria is PGN. The most prominent PGN is the substitution of about 50% of the disaccharides (N-acetylglucan) with muramic acid δ-lactam residue, which occurs predominantly at every alternate disaccharide (Atrih et al., 1996). In this study, the concentration of PGN disaccharides was 43.85% (data not shown). The purification procedure of PGN isolated from *L. acidophilus* was first identified by HPLC (Fig. 2) and Aminex HPX-87H column, which is specific for the isolation of PGN. Compared with PGN from *B. subtilis*, the retention time of *L. acidophilus* was a little longer (Fig. 2D). Chromatographic retention times may be influenced by a number of parameters, including amino acid composition, the nature of the N- and C-terminal residues, peptide length, and peptide sequence (Mant, Kovacs, Kim, Pollock, & Hodges, 2009). Previous studies have also revealed that cell walls can be specifically degraded by lysozyme (glycoside hydrolase) during cell growth (Rae, Geissler, Adamson, & Portnoy, 2011). By comparing the NAG fragment (14.049 min) and NAM (12.255 min) to that generated by the lysozyme digestion of whole PGN (Fig. 2E), a peak retention time at 14.044 min occurred in the hydrolysates of PGN from *L. acidophilus*, which corresponds to the NAG fragment (14.049 min). Other peaks were not identified in Fig. 2E, which may be due to NAM residues that have a peptide stem (not specific to lysozyme), such as tetrapeptides or pentapeptides attached to the D-lactyl moiety (Meroueh et al., 2006). Un-hydrolyzed soluble PGN is shown in Fig. 2F, which showed the same outcome as PGN from *L. acidophilus* (Fig. 2D).

Despite possible problems related to PGN insolubility, various approaches were used to gain insight into the composition of PGN (Fig. 3). $^1$H NMR of the PGN fraction indicated that the structural features of PGN include polysaccharide chains having alternating (β-1,4)-linked NAG-NAM residues. Given PGN insolubility, however, $^1$H NMR was not as suitable in analyzing PGN's structure as some other approaches. Even so, this result showed the presence of a (β-1,4)-linked bond in PGN; therefore the structure of PGN is more complex than predicted (Fig. 2B) (Mulloy, Mourao, & Gray, 2000). We also observed results related to FT-IR. In the 1200–800 cm$^{-1}$ region, multivariate analysis was performed to characterize PGN and differentiate it from other polysaccharides. A C=O stretching vibration band of the amide group was seen at 1650 cm$^{-1}$. N—H deformation and a C—N mixture of amide II occurred at 1540 cm$^{-1}$. These data suggest the existence of tetrapeptide stems substituted in the NAM residues. An O—H absorption band at 3420 cm$^{-1}$, a N—H absorption band at 3300 cm$^{-1}$, a —CH2 asymmetric band at 2930 cm$^{-1}$ and a C—O—C band at 1070 cm$^{-1}$ represented the polysaccharide residues (probably NAG-(β-1,4)-NAM) in this sample. The strong absorption peak at 3300 cm$^{-1}$ may also represent peptide stems substituted in the NAM residues, according to the elucidation by Kacurakova and Wilson (2001). MALDI-TOF/TOF MS analysis showed that the molecular mass of major PGN oligosaccharides was in the 800–900 *m*/*z* range. According to PGN from *B. subtilis*, the molecular mass of water-soluble PGN is 875.260 Da, and the arrows in the PGN structure indicate fragmentation sites (Fig. 3E and Table 1).

**Table 1**
MALDI-MS TOF/TOF analysis of PGN derived from *L. acidophilus*.

| PGN | Ion | *m*/*z* | | Δ*m* | Peptides composition | | | | |
|---|---|---|---|---|---|---|---|---|---|
| | | Observed | Calculated | | Ala | Glu | Lys | Ala | Gly |
| 1 | [M+H]$^+$ | 828.452 | 805.160 | 23(Na) | 1 | 1 | 1 | 0 | 0 |
| 2 | [M+H]$^+$ | 860.283 | 876.283 | 16(O) | 1 | 1 | 1 | 1 | 0 |
| 3 | [M+H]$^+$ | 876.260 | 875.260 | 1(H) | 1 | 1 | 1 | 1 | 0 |
| 4 | [M+H]$^+$ | 892.244 | 876.244 | 16(O) | 1 | 1 | 1 | 1 | 0 |

Chemical analysis of the extracellular polysaccharide confirmed its molecular mass (875.260 Da), the presence of residues of NAG and probably a NAG-(β-1,4)-NAM band in PGN. However, whether this information was accurate in relation to PGN structure could not be confirmed. Nonetheless, the results obtained with CFW and FITC provided more information about PGN structure (Fig. 3F). CFW was used to diagnose and identify the chitinaceous fungal structures, which can bind to the β-1,3 or β-1,4 polysaccharides, such as cellulose and chitin in fungi (Rasconi, Jobard, Jouve, & Sime-Ngando, 2009). The image in Fig. 3F-CFW provides confirmation of β-glucan in PGN succulus. PGN was also alkali-insoluble (data not shown); the same conclusion found for all β-glucans, which are alkali-insoluble (Johansson, Tuomainen, Ylinen, Ekholm, & Virkki, 2004). FITC is specific for lysine; it was covalently linked to the end of the peptides via lysine (Lei, Remy, Labrugere, & Durrieu, 2012). The amino acid analysis shown in Fig. 3A indicates that this fraction contained lysine. Based on the image in Fig. 3F-FITC, it was determined that the PGN biofilm contained lysine residue, which is in keeping with the hypothesis (see MS analysis) that it is a lysine residue tetrapeptide (Jullian et al., 2009).

HPLC, NMR, FT-IR discovery, MALDI-TOF/TOF MS and the amino acid analysis of PGN provided strong evidence about the presumed PGN structure. The molecular mass of PGN from *L. acidophilus* is consistent with NAG-(β-1,4)-NAM-L-Ala-D-Glu-L-Lys-D-Ala.

Comparing Fig. 4-CFW with Fig. 4-FITC, epifluorescence microscopy images provided an excellent illustration of the phagocytosis processes of RAW 264.7 cells engulfing PGN sacculus during LPS induction. The ability of LAB to act as a probiotic agent has been taken advantage of in different foods products. *L. casei* and *L. acidophilus* have been used to defend against many pathological conditions and diseases (Amdekar et al., 2012). *L. sakei* and *L. lactis* could be used to control the foodborne enterobacteriaceae pathogen *E. coli* ATCC8739 (Hequet et al., 2009). *E. coli* can spread to humans through the food chain, posing a potential risk to human health (Johnson et al., 2007). So far, many researchers have focused on lactic acid, which were probably the main molecules implicated in the anti-enterobacterial effect. To our knowledge, the mechanisms causing the reductions in *E. coli* infections shown by *L. acidophilus* are still unknown. Macrophages are professional phagocytes that can engulf microorganisms, tissue

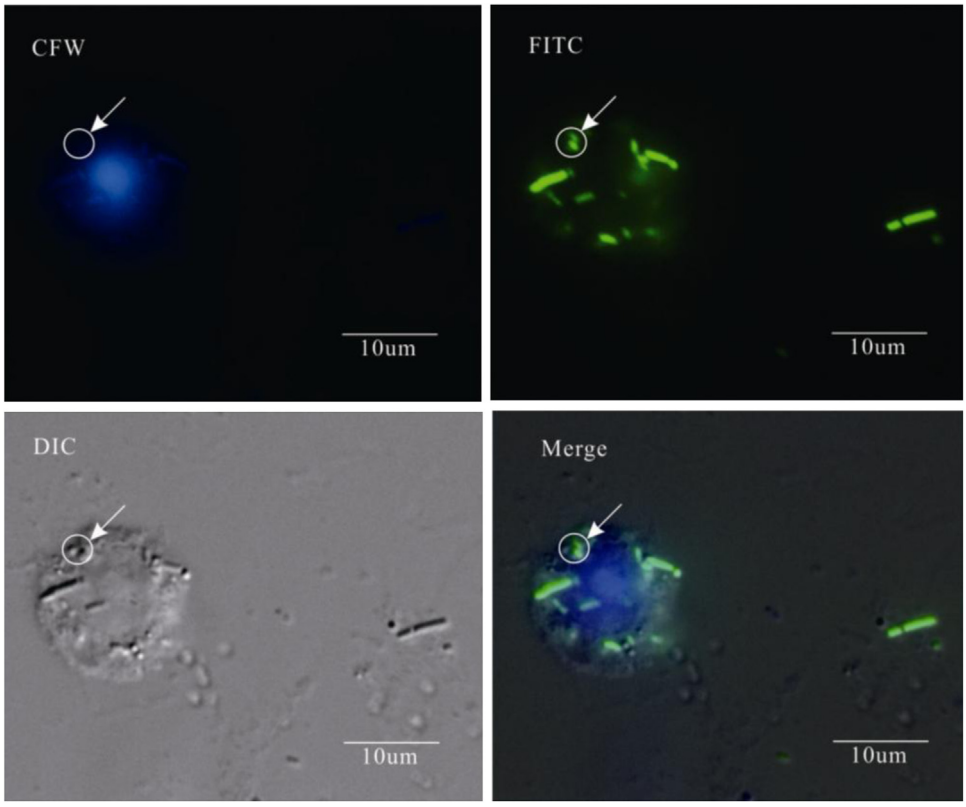


**Fig. 4.** RAW 264.7 cells treated with PGN succulus, PGN was pre-labeled with FITC (outer and inner cell) before cell was treated. PGN was also labeled with CFW (outer cell) 12 h later, and visualized using a Zeiss fluorescence microscope.

debris and apoptotic cells, performing protective and purification functions in tissue repair. Given that *E. coli*-free LPS induces inflammatory responses and contributes to chronic inflammation and tissue injury, we adopted LPS-induced macrophages to study PGN's anti-inflammatory capacity (Palmer et al., 2011). iNOS and COX-2 play a key role in inflammatory responses. As shown in Fig. 5, we found a significant decrease in iNOS and COX-2 protein levels when PGN was added in concentrations up to 200 μg/ml. The cause of the significant role of both of the proteins in the inflammatory response indicated that PGN has a potential anti-inflammatory capacity on LPS-induced macrophages (Fig. 6). At the same time, the effect of PGN on the viability of RAW 264.7 cells was not affected; viability went, from 97.22% to 80.18%, which showed that cell growth was not seriously affected.

PGN derived from *L. acidophilus* demonstrated a potential role in response to LPS-induced macrophages. Comparison of the structure of PGNs of varies kinds of microorganisms showed that the difference in the third amino acid (L-lysine and Meso-$A_2$pm) may

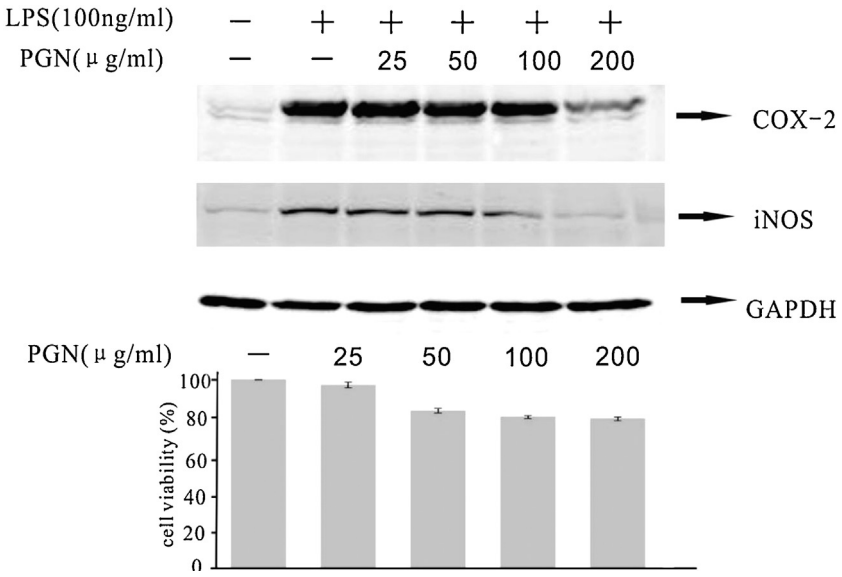


**Fig. 5.** PGN dose-dependently prevents LPS up-regulated iNOS and COX-2 protein levels in RAW 264.7 cells.

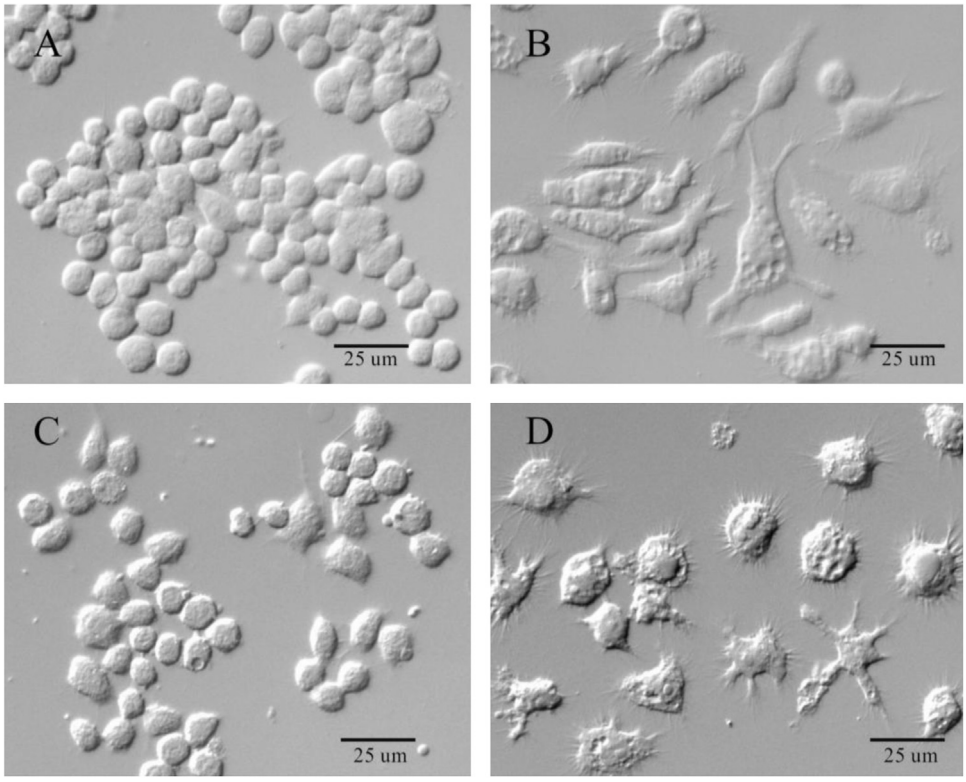


**Fig. 6.** DIC image of RAW 264.7 cells with different treatments for 24 h. (A) Normal RAW 264.7 cells without treatment. (B) RAW 264.7 cells incubated with LPS (100 ng/ml). (C) RAW 264.7 cells incubated with PGN (200 μg/ml). (D) Both LPS and PGN were present in the RAW 264.7 cells.

play a crucial role in the anti-inflammatory capacity of PGN on LPS-induced RAW 264.7 cells. More work needs to be done to determine the mechanism by which PGN acts on RAW 264.7 cells. Based on the composition of PGN, further investigation should focus on the effects of monosaccharides, such as NAG and NAM-tetrapeptides of PGN, and on the up-stream factors related to inflammatory macrophages in order to gain more details about probiotic bacteria and their effector molecules.

## Acknowledgments

This work was supported by the Natural Science Funding of China (41276121 and 31101314) and Zhejiang Province (Z3110211), the Science and Technology Department of Ningbo (2012B82017 and 2011C11017), and the K. C. Wong Magna Fund at Ningbo University.

## References

Atrih, A., Bacher, G., Allmaier, G., Williamson, M. P., & Foster, S. J. (1999). Analysis of peptidoglycan structure from vegetative cells of *Bacillus subtilis* 168 and role of PBP 5 in peptidoglycan maturation. *Journal of Bacteriology*, *181*, 3956–3966.

Atrih, A., Zöllner, P., Allmaier, G., & Foster, S. J. (1996). Structural analysis of *Bacillus subtilis* 168 endospore peptidoglycan and its role during differentiation. *Journal of Bacteriology*, *178*, 6173–6183.

Aly, S. M., Abdel-Galil Ahmed, Y., Abdel-Aziz Ghareeb, A., & Mohamed, M. F. (2008). Studies on *Bacillus subtilis* and *Lactobacillus acidophilus*, as potential probiotics, on the immune response and resistance of *Tilapia nilotica* (*Oreochromis niloticus*) to challenge infections. *Fish Shellfish Immunol*, *25*, 128–136.

Amdekar, S., Roy, P., Singh, V., Kumar, A., Singh, R., & Sharma, P. (2012). Anti-inflammatory activity of *Lactobacillus* on carrageenan-induced paw edema in male wistar rats. *International Journal of Inflammation*, *2012*, 1–6.

Calamita, H. G., Ehringer, W. D., Koch, A. L., & Doyle, R. J. (2001). Evidence that the cell wall of *Bacillus subtilis* is protonated during respiration. *Proceedings of the National Academy of Sciences of the United States of America*, *98*, 15260–15263.

Chambery, A., del Monaco, G., Di Maro, A., & Parente, A. (2009). Peptide fingerprint of high quality Campania white wines by MALDI-TOF mass spectrometry. *Food Chemistry*, *113*, 1283–1289.

Chaput, C., & Boneca, I. G. (2007). Peptidoglycan detection by mammals and flies. *Microbes and Infection*, *9*, 637–647.

Domenech, M., Garcia, E., Prieto, A., & Moscoso, M. (2012). Insight into the composition of the intercellular matrix of *Streptococcus pneumoniae* biofilms. *Environmental Microbiology* [early view].

Dworzanski, J. P., Tripathi, A., Snyder, A. P., Maswdeh, W. M., & Wick, C. H. (2005). Novel biomarkers for Gram-type differentiation of bacteria by pyrolysis–gas chromatography–mass spectrometry. *Journal of Analytical and Applied Pyrolysis*, *73*, 29–38.

Ebrahimi, M. T., & Jafarei, P. (2011). *Lactobacillus acidophilus* cell structure and application. *African Journal of Microbiology Research*, *5*, 4033–4042.

Florez, A. B., Ammor, M. S., Mayo, B., van Hoek, A. H., Aarts, H. J., & Huys, G. (2008). Antimicrobial susceptibility profiles of 32 type strains of *Lactobacillus*, *Bifidobacterium*, *Lactococcus* and *Streptococcus* spp. *International Journal of Antimicrobial Agents*, *31*, 484–486.

Girardin, S. E., Boneca, I. G., Carneiro, L. A. M., Antignac, A., Jehanno, M., Viala, J., & Tedin, K. (2003). Nod1 detects a unique muropeptide from Gram-negative bacterial peptidoglycan. *Science*, *300*, 1584–1587.

Hayhurst, E. J., Kailas, L., Hobbs, J. K., & Foster, S. J. (2008). Cell wall peptidoglycan architecture in *Bacillus subtilis*. *Proceedings of the National Academy of Sciences of the United States of America*, *105*, 14603–14608.

Hequet, A., Laffitte, V., Brocail, E., Aucher, W., Cenatiempo, Y., Frere, J., Fremaux, C., & Berjeaud, J. M. (2009). Development of a new method for the detection of lactic acid bacteria capable of protecting ham against *Enterobacteriaceae*. *Letters in Applied Microbiology*, *48*, 668–674.

Johnson, J. R., Sannes, M. R., Croy, C., Johnston, B., Clabots, C., Kuskowski, M. A., Bender, J., Smith, K. E., Winokur, P. L., & Belongia, E. A. (2007). Antimicrobial drug-resistant *Escherichia coli* from humans and poultry products, Minnesota and Wisconsin, 2002–2004. *Emerging Infectious Diseases*, *13*, 838–846.

Johansson, L., Tuomainen, P., Ylinen, M., Ekholm, P., & Virkki, L. (2004). Structural analysis of water-soluble and -insoluble β-glucans of whole-grain oats and barley. *Carbohydrate Polymers*, *58*, 267–274.

Jullian, M., Hernandez, A., Maurras, A., Puget, K., Amblard, M., Martinez, J., & Subra, G. (2009). N-terminus FITC labeling of peptides on solid support: The truth behind the spacer. *Tetrahedron Letters*, *50*, 260–263.

Kacurakova, M., & Wilson, R. H. (2001). Developments in mid-infrared FT-IR spectroscopy of selected carbohydrates. *Carbohydrate Polymers*, *44*, 291–303.

Kang, J., Zhang, Y., Cao, X., Fan, J., Li, G., Wang, Q., Diao, Y., Zhao, Z., Luo, L., & Yin, Z. (2012). Lycorine inhibits lipopolysaccharide-induced iNOS and COX-2 up-regulation in RAW264.7 cells through suppressing P38 and STATs activation and increases the survival rate of mice after LPS challenge. *International Immunopharmacology*, *12*, 249–256.

Lei, Y., Remy, M., Labrugere, C., & Durrieu, M. C. (2012). Peptide immobilization on polyethylene terephthalate surfaces to study specific endothelial cell adhesion,

spreading and migration. *Journal of Materials Science: Materials in Medicine*, *23*, 2761–2772.

Mant, C. T., Kovacs, J. M., Kim, H. M., Pollock, D. D., & Hodges, R. S. (2009). Intrinsic amino acid side-chain hydrophilicity/hydrophobicity coefficients determined by reversed-phase high-performance liquid chromatography of model peptides: Comparison with other hydrophilicity/hydrophobicity scales. *Biopolymers*, *92*, 573–595.

Maragkoudakis, P. A., Chingwaru, W., Gradisnik, L., Tsakalidou, E., & Cencic, A. (2010). Lactic acid bacteria efficiently protect human and animal intestinal epithelial and immune cells from enteric virus infection. *International Journal of Food Microbiology*, *141*(Suppl. 1), S91–S97.

McPherson, D. C., & Popham, D. L. (2003). Peptidoglycan synthesis in the absence of class A penicillin-binding proteins in *Bacillus subtilis*. *Journal of Bacteriology*, *185*, 1423–1431.

Meisen, S., Wingender, J., & Telgheder, U. (2008). Analysis of microbial extracellular polysaccharides in biofilms by HPLC, Part I: Development of the analytical method using two complementary stationary phases. *Analytical and Bioanalytical Chemistry*, *391*, 993–1002.

Meroueh, S. O., Bencze, K. Z., Hesek, D., Lee, M., Fisher, J. F., Stemmler, T. L., & Mobashery, S. (2006). Three-dimensional structure of the bacterial cell wall peptidoglycan. *Proceedings of the National Academy of Sciences of the United States of America*, *103*, 4404–4409.

Mulloy, B., Mourao, P. A. S., & Gray, E. (2000). Structure:function studies of anticoagulant sulphated polysaccharides using NMR. *Journal of Biotechnology*, *77*, 123–135.

Ng, E. W., Yeung, M., & Tong, P. S. (2011). Effects of yogurt starter cultures on the survival of *Lactobacillus acidophilus*. *International Journal of Food Microbiology*, *145*, 169–175.

O'Flaherty, S. J., & Klaenhammer, T. R. (2010). Functional and phenotypic characterization of a protein from *Lactobacillus acidophilus* involved in cell morphology, stress tolerance and adherence to intestinal cells. *Microbiology*, *156*, 3360–3367.

Palmer, C. D., Mancuso, C. J., Weiss, J. P., Serhan, C. N., Guinan, E. C., & Levy, O. (2011). 17(R)-Resolvin D1 differentially regulates TLR4-mediated responses of primary human macrophages to purified LPS and live *E. coli*. *Journal of Leukocyte Biology*, *90*, 459–470.

Rae, C. S., Geissler, A., Adamson, P. C., & Portnoy, D. A. (2011). Mutations of the *Listeria monocytogenes* peptidoglycan N-deacetylase and O-acetylase result in enhanced lysozyme sensitivity, bacteriolysis, and hyperinduction of innate immune pathways. *Infection and Immunity*, *79*, 3596–3606.

Rasconi, S., Jobard, M., Jouve, L., & Sime-Ngando, T. (2009). Use of calcofluor white for detection, identification, and quantification of phytoplanktonic fungal parasites. *Applied and Environmental Microbiology*, *75*, 2545–2553.

Semjonovs, P., Jasko, J., Auzina, L., & Zikmanis, P. (2008). The use of exopolysaccharide-producing cultures of latic acid baceria to improve the functional value of fermented foods. *Journal of Food Technology*, *6*, 101–109.

Shah, I. M., Laaberki, M. H., Popham, D. L., & Dworkin, J. (2008). A eukaryotic-like Ser/Thr kinase signals bacteria to exit dormancy in response to peptidoglycan fragments. *Cell*, *135*, 486–496.

Shih, M. F., Cheng, Y. D., Shen, C. R., & Cherng, J. Y. (2010). A molecular pharmacology study into the anti-inflammatory actions of *Euphorbia hirta* L. on the LPS-induced RAW 264.7 cells through selective iNOS protein inhibition. *Journal of Natural Medicines*, *64*, 330–335.

Travassos, L. H., Girardin, S. E., Philpott, D. J., Blanot, D., Nahori, M. A., Werts, C., & Boneca, I. G. (2004). Toll-like receptor 2-dependent bacterial sensing does not occur via peptidoglycan recognition. *EMBO Reports*, *5*, 1000–1006.

Vissers, Y. M., Snel, J., Zuurendonk, P. F., Smit, B. A., Wichers, H. J., & Savelkoul, H. F. (2010). Differential effects of *Lactobacillus acidophilus* and *Lactobacillus plantarum* strains on cytokine induction in human peripheral blood mononuclear cells. *FEMS Immunology and Medical Microbiology*, *59*, 60–70.

Weiss, G., Rasmussen, S., Zeuthen, L. H., Nielsen, B. N., Jarmer, H., Jespersen, L., & Frokiaer, H. (2010). *Lactobacillus acidophilus* induces virus immune defence genes in murine dendritic cells by a Toll-like receptor-2-dependent mechanism. *Immunology*, *131*, 268–281.

Zapun, A., Noirclerc-Savoye, M., Helassa, N., & Vernet, T. (2012). Peptidoglycan assembly machines: The biochemical evidence. *Microbial Drug Resistance*, *18*, 256–260.